NUMERICAL INVESTIGATION OF THE CAVITATIONAL BEHAVIOR OF A STORAGE PUMP

Adrian STUPARU*

Department of Hydraulic Machines, "Politehnica" University of Timisoara, Romania

Sebastian MUNTEAN

Centre of Advanced Research in Engineering Sciences, Romanian Academy - Timisoara Branch, Romania

Romeo SUSAN-RESIGA

Department of Hydraulic Machines, "Politehnica" University of Timisoara, Romania

Liviu ANTON

Department of Hydraulic Machines, "Politehnica" University of Timisoara, Romania

ABSTRACT

This paper presents the numerical investigation of the 3D multiphase flow in the impeller of a centrifugal pump from a pumping station by using commercial code FLUENT 6.3. The storage pump has five blades and it is operating at a certain flow rate with a given rotational speed. The computational domain represents only one inter blade channel of the impeller and was generated using the pre-processor GAMBIT from FLUENT, based on the existing geometry. A steady relative 3D multiphase flow is computed in the 3D computational domain and the numerical solution of flow equations is obtained with the expert code FLUENT 6.3, using a Reynolds-Averaged Navier-Stokes (RANS) solver. In order to solve the multiphase flow, the mixture model of the solver is used.

KEYWORDS

storage pump, 3D numerical investigation, mixture model, cavitational flow.

1. INTRODUCTION

In many engineering applications, cavitation has been the subject of extensive theoretical and experimental research since it has predominantly been perceived as an undesirable phenomenon. This is mainly due to the detrimental effects of cavitation such as erosion, noise and vibrations, caused by the growth and collapse of vapour bubbles. The ability to model cavitating flows has drawn strong interest in CFD community. It covers a wide range of applications, such as pumps, hydraulic turbines, inducers and fuel cavitation in orifices as commonly encountered in fuel injection systems. Fluid machinery is a common application where low pressures are routinely generated by the machine action, e.g. on blade surfaces, with a consequent possibility of cavitation. Existence of cavitation is often undesired, because it can degrade the device performance, produce undesirable noise, lead to physical damage to the device and affect the structural integrity. Details of the existence,

* *Corresponding author:* Department of Hydraulic Machinery, „Politehnica" University of Timisoara, Romania, phone: +40 256 403698, fax: +40 256 403698, email: astuparu@mh.mec.upt.ro

extent and effects of cavitation can be of significant help during the design stages of fluid machinery, in order to minimize cavitation or to account for its effects and optimize the design.

Past several decades have seen considerable research on cavitation and extensive reviews are available in the literature [1], [3]. Different aspects of this complex phenomenon have been explored, including, e.g., cavitation bubble collapse and erosion damage, cavitation acoustics, cloud cavitation and rotating cavitation.

Viscous flow models, which regard the cavitating flow as the bubbly flow containing spherical bubbles, were introduced to provide highly accurate calculations. In the viscous flow models, the Navier-Stokes equation including cavitation bubble is solved in conjunction with Rayleigh's equation governing the change in the bubble radius. To account for the cavitation dynamics in a more flexible manner a transport equation model has been developed. In this approach volume or mass fraction of liquid (and vapour) phase is convective. Singhal et al. [5], have employed similar models based on this concept with differences in the source terms.

This paper presents the computational analysis of the cavitational behaviour of a storage pump. Two-phase cavitating flow models based on homogeneous mixture approach, with a transport equation for the vapour volume fraction have been included in expert commercial codes such as FLUENT [6]. We conclude that, for steady cavitating flow, the model presented in this paper, captures correctly the vapour phase distribution on the blade of the pump impeller. The current effort is based on the application of the full cavitation model that utilizes the modified Rayleigh-Plesset equations for bubble dynamics and includes the effects of turbulent pressure fluctuations and non-condensable gases (ventilated cavitation) to rotating cavitation in different types of fluid turbomachines.

2. NUMERICAL METHOD OF MODELING CAVITATING FLOW

The FLUENT code employs a generally applicable predictive procedure for turbulent two-phase cavitating flows developed by Coklja t et al. [3]. This model enables formation of vapour from liquid when the pressure drops below the vaporization pressure. If α_V is the vapour volume fraction, then the continuity equation for the vapour phase is,

$$\frac{\partial}{\partial t}\left(\alpha_V \rho_V\right) + \nabla \cdot \left(\alpha_V \rho_V \vec{u}_V\right) = \dot{m}_V \tag{1}$$

where $\vec{u}_V$ is the velocity of the vapour phase, ρ_V is the vapour density, and $\dot{m}_V$ is the rate of liquid-vapour mass transfer. Obviously, the liquid volume fraction is

$$\alpha_l = 1 - \alpha_V \tag{2}$$

and the mixture density and viscosity are:

$$\rho_m = \left(1 - \alpha_V\right)\rho_l + \alpha_V \rho_V \tag{3}$$

$$\mu_m = \left(1 - \alpha_V\right)\mu_l + \alpha_V \mu_V \tag{4}$$

The continuity equation for the liquid phase is:

$$\frac{\partial}{\partial t}\left(\alpha_l \rho_l\right) + \nabla \cdot \left(\alpha_l \rho_l \vec{u}_l\right) = -\dot{m}_V \tag{5}$$

Adding Eq.(5) to Eq.(1) the mixture continuity equation is obtained:

$$\frac{\partial \rho_m}{\partial t} + \nabla \cdot \left(\rho_m \vec{u}_m\right) = 0 \tag{6}$$

where the mixture velocity is defined by:

$$\rho_m \vec{u}_m = \left(1 - \alpha_V\right)\rho_l \vec{u}_l + \alpha_V \rho_V \vec{u}_V \tag{7}$$

Assuming homogeneous multiphase flow, with no slip between the phases, the same velocity field is shared among the phases:

$$\vec{u}_m = \vec{u}_V = \vec{u}_l \tag{8}$$

This assumption is motivated in the cavitation model because no interface between the liquid and vapour phases is assumed, thus allowing the fluids to be interpenetrating. The conservation equation for momentum (with negligible body forces) is:

$$\frac{\partial}{\partial t}\left(\rho_m \vec{u}_m\right) + \nabla \cdot \left(\rho_m \vec{u}_m \vec{u}_m\right) = -\nabla p_m + \nabla \cdot \mu_m \left[\nabla \vec{u}_m + \left(\nabla \vec{u}_m\right)^T\right] \tag{9}$$

Since the cavitation bubble grows is a liquid at low temperature the latent heat of evaporation can be neglected and the system can be considered isothermal. Under these conditions the pressure inside the bubble remains practically constant and the growth of the bubble radius, *R*, can be approximated by the simplified Rayleigh equation:

$$\frac{dR}{dt} = \sqrt{\frac{2\left(p_{vap} - p\right)}{3\rho_l}} \tag{10}$$

where p_{vap} is the pressure of vaporization and ρ_l is the liquid density. The total mass of vapour per mixture volume unit can be written as:

$$m_V = \rho_V \frac{4}{3}\pi R^3 n_b \tag{11}$$

with n_b is the bubble number density. It results,

$$\dot{m}_V = \frac{dm_V}{dt} = \frac{3\rho_V \alpha_V}{R}\frac{dR}{dt} = \frac{3\rho_V \alpha_V}{R}\sqrt{\frac{2\left(p_{vap} - p\right)}{3\rho_l}} \tag{12}$$

with bubble radius given by:

$$R = \left(\frac{\alpha_V}{\frac{4}{3}\pi n_b}\right)^{1/3} \tag{13}$$

Bernad et al. [2] suggest a minimum of 10^4 and maximum of 10^6 values for the bubble density number n_b. However, in [2] it shows that the bubble initial radius has an insignificant influence on the final radius, as well as on the time for bubble growing up along streamlined bodies. As a result, when a steady cavitating flow configuration is computed, the bubble density number should have little influence on the final result.

The FLUENT code requires the following methodology for computing cavitating flows. First, a steady solution is obtained for a single phase (liquid) flow, solving Eq.(6) and Eq.(9). Second, the cavitation model is turned on and the steady equations are solved, with the vapour volume fraction, and therefore the liquid-vapour mixture density, as an additional unknown.

Physically, the cavitation process is governed by thermodynamics and kinetics of the phase change process.

The liquid-vapour conversion associated with the cavitation process is modelled through two terms, which represents, respectively, condensation and evaporation.

3. NUMERICAL APPROACH, COMPUTATIONAL DOMAIN AND BOUNDARY CONDITIONS

To simulate the cavitating flow the numerical code FLUENT [6] was used. The code uses a control volume-based technique to convert the governing equations in algebraic

equations that can be solved numerically. This control volume technique consists of integrating the governing equations at each control volume, yielding discrete equations that conserve each quantity on a control-volume basis. The governing integral equations for the conservation of mass and momentum, and (when appropriate) other scalars, such as turbulence, are solved sequentially. Being the governing equations non-linear (and coupled), several iterations of the solution loop must be performed before a converged solution is obtained. The flow solution procedure is the SIMPLE routine [6]. This solution method is designed for incompressible flows, thus being implicit. The full Navier-Stokes equations are solved. The flow was assumed to be steady, and isothermal. In these calculations turbulence effects were considered using turbulence models, as the k-ε RNG models, with the modification of the turbulent viscosity for multiphase flow. To model the flow close to the wall, enhanced wall functions approach has been used to model the near-wall region (i.e., laminar sub layer, buffer region, and fully-turbulent outer region). For this model, the used numerical scheme of the flow equations was the segregated implicit solver. The SIMPLE scheme was employed for pressure-velocity coupling, first-order up-wind for the momentum equations and for other transport equations (e.g. vapour transport and turbulence modelling equations). Computational domain is meshed using the GAMBIT pre-processor [6].

The computational domain includes the impeller of the storage pump. For the numerical investigation only one inter-blade channel is used because of the symmetry of the geometry, Fig.1.

Fig.1 Impeller of the storage pump with highlighted inter blade channel

The inter-blade channel domain is meshed with 322726 cells using a structured mesh, see Fig.2.

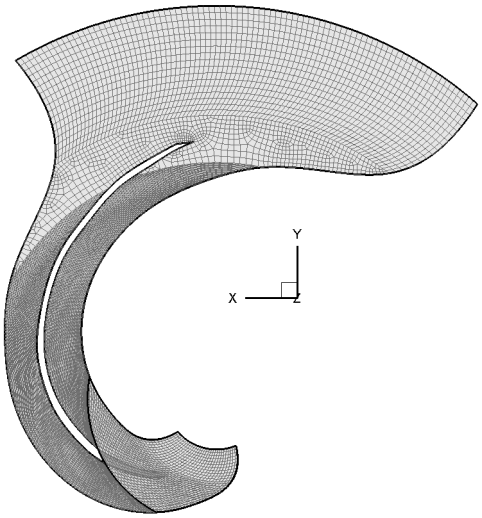

Fig.2 Mesh generated on the 3D computational domain of the inter-blade channel

On the inlet surface of the impeller, for the liquid phase, a constant velocity field was imposed normal on the surface. The velocity magnitude is computed using the flow rate of the operating point:

$$v_{l\_IN} = \frac{Q}{S_{IN}} \tag{14}$$

On the outlet surface a constant value of the pressure is imposed. Then, the pressure is lowered slowly down to the value corresponding to the desired cavitation number σ defined as:

$$\sigma = \frac{p_{m\_IN} - p_{vap}}{\rho_m g H} \tag{15}$$

Vapour appears during the pressure decrease. After obtaining a steady single phase (liquid) flow solution, FLUENT 6.3 code allows turning on the cavitation model. As a consequence, vapour formation is enabled where the absolute pressure is smaller than the vaporization pressure, p_{vap}. In order to obtain correct results the operating pressure, p_{op}, must be set to zero (by default is equal with the atmospheric pressure), therefore the gauge pressure, p_{gauge}, will be equal with the absolute pressure, p_{abs}:

$$p_{abs} = p_{op} + p_{gauge} \tag{16}$$

This setting is important for obtaining only positive absolute pressure values.

On the periodic surfaces of the impeller the periodicity of the velocity, pressure and turbulence parameters were imposed:

$$p(r,\theta,z) = p\left(r,\theta+\frac{2\pi}{n_p},z\right) \tag{17}$$

$$\vec{v}(r,\theta,z) = \vec{v}\left(r,\theta+\frac{2\pi}{n_p},z\right) \tag{18}$$

$$k(r,\theta,z) = k\left(r,\theta+\frac{2\pi}{n_p},z\right) \tag{19}$$

$$\varepsilon(r,\theta,z)=\varepsilon\left(r,\theta+\frac{2\pi}{n_p},z\right) \tag{20}$$

The remaining boundary conditions for the impeller domain correspond to zero relative velocity on the blade, crown and hub.

Fig.3 shows the 3D computational domain with boundary conditions corresponding to an inter-blade channel of the impeller. The computational domain is bounded upstream by an annular section (wrapped on the same annular surface as the suction outlet section, but different in angular extension) and extends downstream up to cylindrical patch, in order to impose the boundary conditions on the outlet section.

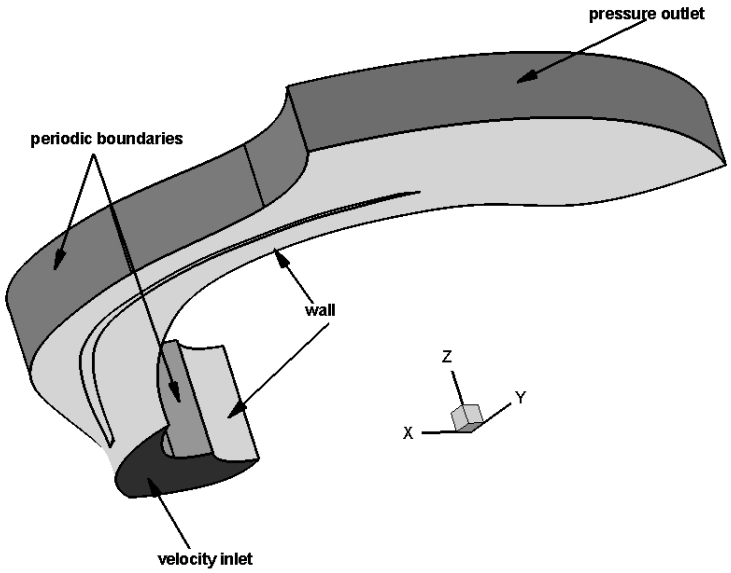

Fig.3 Boundary conditions on the computational domain

We investigated the storage pump operating only on the best efficiency point with the characteristics given in the Tab.1:

Parameter	Symbol	Value
Rotational speed	n, [rot/min]	1500
Flow rate	Q, [m^3/s]	1.012
Pumping head	H, [m]	319

Tab.1 Values of the main characteristics of the best efficiency point

4. NUMERICAL RESULTS

In order to compute the pumping head the following equation is used:

$$H=\frac{p_{m\_OUT}-p_{m\_IN}}{\rho_m g}+\frac{v^2_{m\_OUT}-v^2_{m\_IN}}{2g}+z_{OUT}-z_{IN} \tag{21}$$

If the total pressure is given by:

$$p_{m\_tot} = p_m + \frac{\rho_m v_m^2}{2} \tag{22}$$

and the difference between the inlet and outlet position is negligible then the pumping head has the following expression:

$$H = \frac{p_{m\_tot\_OUT} - p_{m\_tot\_IN}}{\rho_m g} = \frac{\Delta p_{m\_tot}}{\rho_m g} \tag{23}$$

The suction head is determined with the equation:

$$H_s = \frac{p_{atm} - p_{tot\_IN}}{\rho_m g} \tag{24}$$

From the numerical simulation of the multiphase flow for best efficiency operating point of the storage pump we obtained the following results:

Nr.	Q [m^3/s]	p_{tot_IN} [Pa]	p_{tot_OUT} [Pa]	ρ_m [kg/m^3]	H [m]	H_s [m]	σ [-]	V_V [cm^3]
1	1.02	846478.5	2514930	999.98	170.08	-75.96	0.506	0.29
2		836823.19	2504784.8	999.98	170.03	-74.98	0.500	0.33
3		826871.69	2494766.3	999.98	170.02	-73.96	0.494	0.39
4		808278.25	2474214.5	999.97	169.83	-72.07	0.484	0.47
5		790242.88	2453441.8	999.97	169.55	-70.23	0.474	0.59
6		751926.88	2412958.8	999.94	169.33	-66.32	0.451	1.07
7		718620.63	2370118	999.92	168.36	-62.93	0.434	1.39
8		628275.88	2267660	999.8	167.15	-53.73	0.382	3.70
9		582544.19	2214636.8	999.69	166.42	-49.07	0.355	5.79
10		539162.63	2163463.8	999.58	165.65	-44.65	0.330	7.84
11		490994.41	2114397.5	999.32	165.60	-39.75	0.301	12.59
12		456408.63	2045018.5	998.8	162.13	-36.24	0.286	22.17
13		419595.47	2007570.5	998.64	162.09	-32.49	0.263	25.21
14		382920.53	1955235.6	998.07	160.59	-28.76	0.242	35.72
15		363533.22	1898207.8	997.11	156.89	-26.81	0.235	53.50

Tab.2 Numerical results for the multiphase flow inside the storage pump

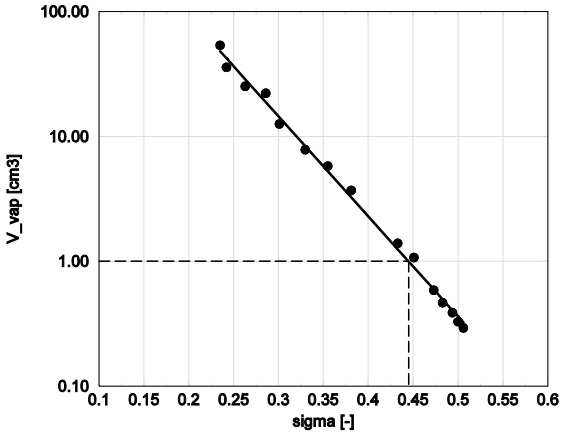

Fig.4 Variation of the volume of vapour against the cavitation number for best efficiency point

In Fig.4 it is represented the variation of the volume of vapour against the cavitation number in a semi-logarithmic plot. In order to determine the cavitation incipience coefficient, it was considered, according to a theory developed by professor Romeo SUSAN-RESIGA, that the volume of vapour of 1 cm^3 corresponds to the cavitation incipience. From Fig.4 it can be observed that the volume of vapour increases while the cavitation number decreases and that the cavitation incipience coefficient is equal with σ_i = 0.444.

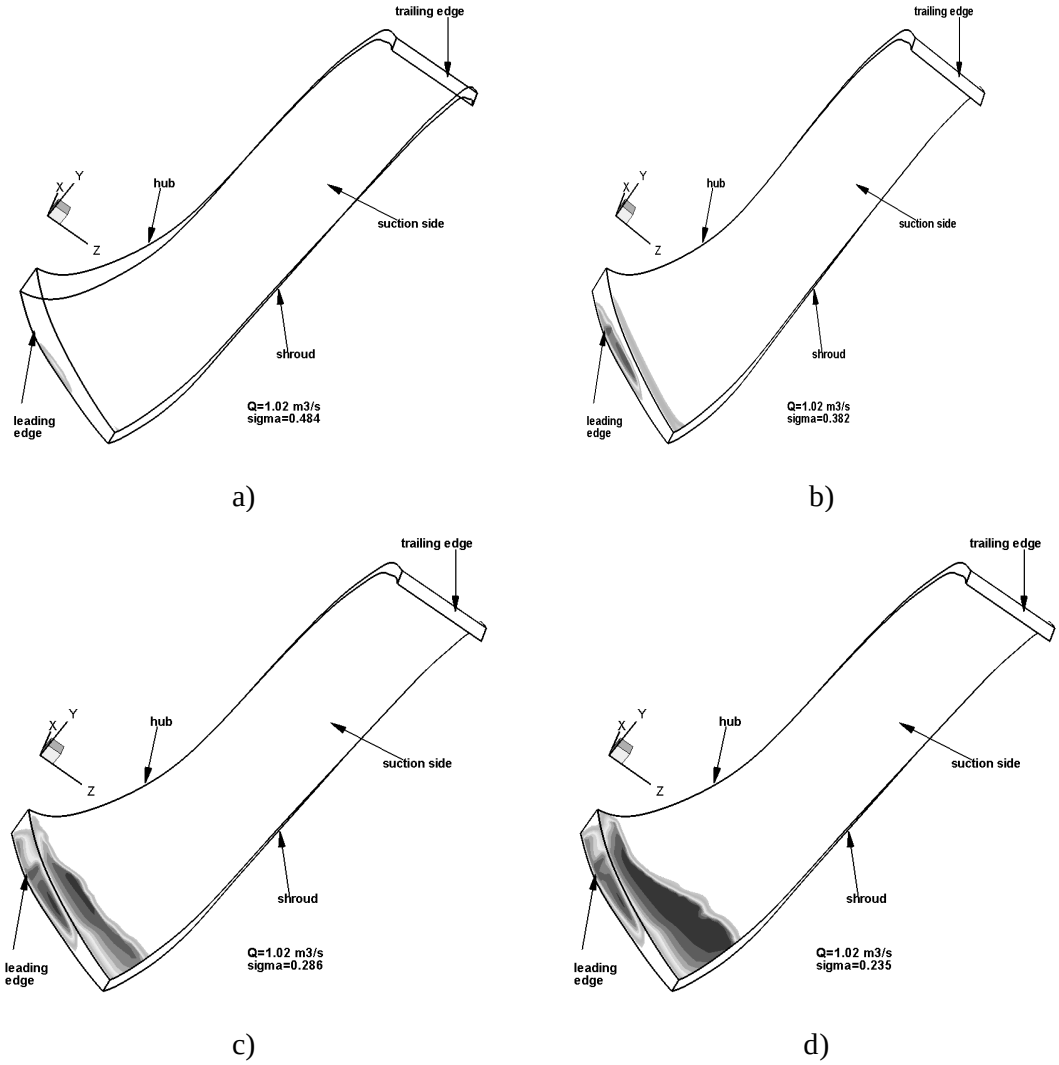

Fig.5 Distribution of the volume of vapour on the suction side of the blade for different cavitation numbers

Analysing Fig.5 and Fig.4 it results that for σ = *0.314*, corresponding to the best efficiency operating point of the storage pump, the cavitation phenomena is present on the suction side of the impeller blade.

From Fig.5 it can be observed that while the suction head is decreasing, so that the contra pressure on the inlet of the pump will be smaller, the cavitation phenomena it develops more and more. Initially, the volume of vapour is present only on the leading edge, but it grows and in the end is present on almost 2/3 of the leading edge and on a great part of the suction side of the blade

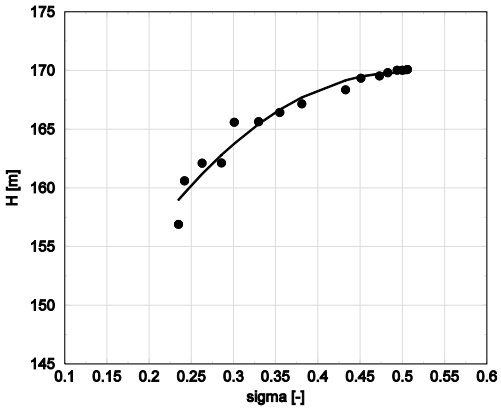

Fig.6 Pumping head drop due to cavitation

In Fig.6 it is presented the evolution of the pumping head corresponding to the decreasing of the cavitation number. It results that the pumping head is dropping abruptly while the cavitation number is getting smaller.

5. CONCLUSION

The analyse of the results of the numerical investigation of the multiphase flow inside the storage pump underlines the pumping head drop due to the development of cavitation phenomena, while the level of the water fro the suction lake drops, even for the best efficiency point. It is obviously that, while the cavern filled with vapour grows, the perturbation of the flow on the suction side of the blade is more accentuated, leading to the detachment of the flow from the blade, the decreasing of the deviation realised by the impeller blades, and consequently to the pumping head drop. On the other hand, the growth of the boundary layer on the suction side of the blade and the detachment of the flow leads to the increase of the hydraulic losses and the decrease of the hydraulic efficiency of the impeller.

The cavitation phenomena appears even on the best efficiency operating point of the pump due to the unfavourable hydrodynamics generated by the geometric shape of the impeller blades, the leading edge of the blades being very sharp. In order to avoid the appearance of cavitation it is necessary to redesign the impeller with modern design methods and software.

6. ACKNOWLEDGEMENTS

The present work has been supported by Romanian Academy program "Hydrodynamics Optimization and Flow Control of the Hydraulic Turbomachinery in order to Improve the Energetic and Cavitational Performances".

7. REFERENCES

[1] Anton, I., *Cavitation* (in Romanian), Romanian Academy Publishing House, Bucharest, 1984 (Vol. 1), 1985 (Vol. 2)

[2] Bernad, S., Resiga, R., Muntean, S., Anton, I., *Cavitation Phenomena in Hydraulic Valves. Numerical Modelling*, Proceeding of the Romanian Academy, Series A, Volume 8, Number 2/2007, The Publishing House of the Romanian Academy, 2007

[3] Cokljat, D., Ivanov, V.A., Vasquez, S.A., *Two-Phase Model for Cavitating Flows*, in Third International Conference on Multiphase Flow, Lyon, France, Available on ICMF98 CD-ROM, paper 224, 1998.

[4] Li S.C., *Cavitation of Hydraulic Machinery*, Imperial College Press, 2000.

[5] Singhal, A. K., Vaidya, N., Leonard, A. D., *Multi-Dimensional Simulation of Cavitating Flows Using a PDF Model for Phase Change*, ASME FED Meeting, Paper No. FEDSM'97-3272, Vancouver, Canada, 1997.

[6] FLUENT 6.3 User's Guide, Fluent Incorporated, 2002.

8. NOMENCLATURE

g	[m/s^2]	gravitational acceleration	α_l	[-]	liquid volume fraction
H	[J/N]	pumping head	α_V	[-]	vapour volume fraction
H_s	[J/N]	suction head	ε	[m^2/s^2]	dissipation rate
k	[m^2/s^2]	turbulent kinetic energy	μ_m	[kg/m.s]	liquid-vapour mixture viscosity
$\dot{m}_V$	[kg/(s.m^{-3})]	rate of liquid-vapour mass transfer	μ_l	[kg/m.s]	liquid volume fractio viscosity
m_V	[kg/(s.m^{-3})]	total mass of vapour per liquid-vapour mixture volume	μ_V	[kg/m.s]	vapour volume fraction viscosity
n	[rot/min]	rotational speed	ρ_m	[kg/m^3]	liquid-vapour mixture volume fraction density
n_b	[1/m^3]	number of bubbles per unit volume of liquid	ρ_l	[kg/m^3]	liquid volume fraction density
n_p	[-]	number of blades	ρ_V	[kg/m^3]	vapour volume fraction density
p_m	[Pa]	liquid-vapour mixture pressure	σ	[-]	cavitation number
p_{m_tot}	[Pa]	liquid-vapour mixture total pressure	σ_i	[-]	cavitation number
p_{abs}	[Pa]	absolute pressure	ϕ	[rad]	angular coordinate
p_{atm}	[Pa]	atmospheric pressure	p_{gauge}	[Pa]	gauge pressure
p_{op}	[Pa]	operating pressure	p_{vap}	[Pa]	vaporization pressure
p_{m_IN}	[Pa]	inlet liquid-vapour mixture pressure	p_{m_OUT}	[Pa]	outlet liquid-vapour mixture pressure
$p_{m\_tot\_IN}$	[Pa]	inlet liquid-vapour mixture total pressure	$p_{m\_tot\_OUT}$	[Pa]	outlet liquid-vapour mixture total pressure
Q	[m^3/s]	flow rate	r	[m]	radial coordinate
R	[m]	bubble radius	t	[s]	time
$\vec{u}_m$	[m/s]	liquid-vapour mixture Velocity	v_{l_IN}	[m/s]	inlet liquid phase velocity
$\vec{u}_l$	[m/s]	liquid phase velocity	v_{m_IN}	[m/s]	inlet liquid-vapour mixture velocity
$\vec{u}_V$	[m/s]	vapour phase velocity	v_{m_OUT}	[m/s]	outlet liquid-vapour mixture velocity
z	[m]	axial coordinate	z_{IN}	[m]	inlet position
z_{OUT}	[m]	outlet position			